

Technical Note

# Mare Volcanism in Apollo Basin Evaluating the Mare Basalt Genesis Models on the Moon

Xiaohui Fu <sup>1,2,\*</sup> , Chengxiang Yin <sup>1</sup>, Jin Li <sup>1</sup>, Jiang Zhang <sup>1</sup> , Siyue Chi <sup>1</sup>, Jian Chen <sup>1</sup>  and Bo Li <sup>1</sup>

<sup>1</sup> Shandong Key Laboratory of Optical Astronomy and Solar-Terrestrial Environment, School of Space Science and Physics, Institute of Space Sciences, Shandong University, Weihai 264209, China; 202017732@mail.sdu.edu.cn (C.Y.); 202317788@mail.sdu.edu.cn (J.L.); zhang\_jiang@sdu.edu.cn (J.Z.); sychi@mail.sdu.edu.cn (S.C.); merchenj@sdu.edu.cn (J.C.); libralibo@sdu.edu.cn (B.L.)

<sup>2</sup> CAS Center for Excellence in Comparative Planetology, Hefei 230026, China

\* Correspondence: fuxh@sdu.edu.cn

**Abstract:** The Apollo basin is a well-preserved double-ringed impact basin located on the northeastern edge of the South Pole–Aitken (SPA) basin. The Apollo basin has been flooded and filled with large volumes of mare lavas, indicating an active volcanism history. Based on orbital data, we reveal that the Apollo basin exhibits an overall asymmetric configuration in the distribution of mare basalts as well as its topography, chemical compositions, and crustal thickness. The Apollo basin is an excellent example for assessing the influences of the above factors on mare basalts petrogenesis and evaluating mare basalt genesis models. It was found that the generation of mare basalt magmas and their emplacement in the Apollo basin seems to be strongly related to local thin crust (<30 km), but the formation of basaltic magmas should be independent of the decompression melting because the mare units (3.34–1.79 Ga) are much younger than the pre-Nectarian Apollo basin. The mare basalts filled in the Apollo basin exhibits a large variation of TiO<sub>2</sub> abundances, indicating the heterogeneity of mantle sources, which is possible due to the lunar mantle overturn after the LMO solidification or the impact-induced mantle convection and migration. However, the prolonged mare volcanic history of the Apollo basin is not well explained, especially considering the low Th abundance (<2 ppm) of this region. In addition, the central mare erupted earlier than other mare units within the Apollo basin, which seems to contradict the predictions of the postbasin loading-induced stresses model. Laboratory investigations of the Chang'E-6 mare basalt samples could possibly answer the above questions and provide new insight into the mare volcanic history of the lunar farside and the connections between mare volcanism and impact basin formation/evolution.

**Keywords:** mare volcanism; magma genesis models; Apollo basin; impact basin



**Citation:** Fu, X.; Yin, C.; Li, J.; Zhang, J.; Chi, S.; Chen, J.; Li, B. Mare Volcanism in Apollo Basin Evaluating the Mare Basalt Genesis Models on the Moon. *Remote Sens.* **2024**, *16*, 4078. <https://doi.org/10.3390/rs16214078>

Academic Editors: Maurizio Pajola, Francesca Esposito, Alice Lucchetti and Simone Pirrotta

Received: 5 September 2024

Revised: 16 October 2024

Accepted: 29 October 2024

Published: 31 October 2024



**Copyright:** © 2024 by the authors. Licensee MDPI, Basel, Switzerland. This article is an open access article distributed under the terms and conditions of the Creative Commons Attribution (CC BY) license (<https://creativecommons.org/licenses/by/4.0/>).

## 1. Introduction

Mare volcanism is a fundamental geological process on the Moon. It could provide insights into the composition of the mantle, the convection process, and lunar thermal history [1]. Mare basalts, as the products of lunar volcanism, cover about 17% of the lunar surface area and contribute less than 1% to the lunar crust volume (on the order of 10<sup>7</sup> km<sup>3</sup>) [2]. Mare basalts are considered to originate by partial melting of the lunar mantle at considerable depths, then move upwards due to excess pressure at or below the crust–mantle boundary as dikes, and finally flood over the lunar surface to produce larger-scale, effusive plains [3–6]. Therefore, lunar mare basalts can be taken as probes of the mantle composition and thermal evolution of the Moon. Unraveling lunar volcanic history is crucial for understanding the mantle composition and thermal evolution of the Moon.

On the basis of lunar sample laboratory analysis and of remote sensing interpretation, a systematic understanding of global distribution patterns, chemical compositions, and volcanic history of mare basalt on the Moon has been built. Different models of mare

basalt genesis have been proposed to explain the volcanism relationship with impact basins, heat sources for melting, and the composition and depth of mantle source regions. However, many outstanding questions concerning lunar mare basalt volcanism are still unanswered. Firstly, the origin for the global asymmetry of lunar mare basalts is still unclear. Remote spectral observations of lunar surface have revealed the fact that mare basalt is primarily concentrated in the large impact basins of the lunar nearside, occurring either in the central portion of multi-ring basins or in troughs concentric to the basin [3,7]. In contrast, only isolated small mare deposits have been found on the far side of the Moon. The hemispherical asymmetry of mare distribution is the first-order of lunar feature, which was thought to be related to lunar crustal thickness asymmetry. But this hypothesis remains to be further verified. Secondly, the duration of lunar mare volcanism has not been well constrained. Radiometric dating of Apollo and Luna mare basalt samples has determined crystallization ages ranging from approximately 4.3–3.1 Ga, and the majority of them formed during the Imbrian period approximately 3.9–3.1 Ga [8,9]. The Chang'E-5 (CE-5) mare basalt as well as some lunar basaltic meteorites (such as Northwest African 773 and 032) extend the recent magmatic activity to 2.0 Ga. However, the surface ages of the mare units derived from crater size–frequency measurements indicate that lunar volcanism was still active until ~1.0 Ga [10,11]. The poorly constrained history of mare volcanism hinders our interpretation of the evolution of the lunar mantle and thermal history of the Moon. Thirdly, mare basalts have substantially large compositional variations (such as  $\text{TiO}_2$  content), indicating mantle source heterogeneities [12,13]. Petrologic and geochemical analyses of mare basalts have revealed their compositional diversity, compared with their terrestrial counterparts. A gravitational overturn of the lunar mantle cumulates has been proposed to explain the  $\text{TiO}_2$  and heat-producing elements' (U, Th, and K) abundances in the source region of mare basalts. However, much of the debate concerning the chemical nature of the lunar mantle, and the heat sources and melting processes, is still going on. In addition, the trending between the  $\text{TiO}_2$  abundance and the mare unit ages in the individual impact basin or on a global scale is still controversial [14–16].

Mare deposits have been found in the Apollo basin, indicating the active mare volcanic history of this region. The Apollo basin is a 538 km wide double-ringed impact structure centered near 36°S, 152°W (Figure 1). The numerical modeling by Potter et al. (2018) indicates that the Apollo basin may be produced by a 40 km diameter body at a speed of 15 km/s, targeting on a 20–40 km thick crust [17]. This impact can possibly penetrate through the ejecta of SPA down to a depth of ~30 km, excavate subcrustal materials, and further expose them in the peak ring of the Apollo basin [17,18]. Dark mare basalts have been found to be flooded in the central, western, and southern portions of the Apollo basin [19–22]. Diverse volcanic landforms, such as wrinkle ridges, sinuous rilles, mare domes, and pyroclastic deposits have been identified as well. Moreover, the Chang'E-6, as a robotic sample return mission, successfully landed on the southern mare unit of the Apollo basin and collected a total of 1935.3 g of lunar soil samples (Figure 1). The coupled investigation of remote sensing data and returned samples could help us understand the mare volcanism of the Apollo basin in depth.

Mare deposits are asymmetrically distributed within the Apollo basin. Meanwhile, the Apollo basin exhibits lateral variations in its mineralogical/chemical compositions, crust thickness, and tectonic setting. It would be valuable to explore the possible link of the above factors to mare volcanism. Therefore, the Apollo basin is an excellent example for assessing the influences of the above factors on mare basalts petrogenesis in a typical impact basin and evaluating mare basalt genesis models, which would further improve our understanding of global mare volcanism. In the present study, we conducted comprehensive chemical, mineralogical, and chronological analyses on the Apollo basin using multiple remote sensing data. We also proposed the potential of CE-6 mare basalts for interpreting the relationship of mare volcanism and impact on basin formation/evolution.

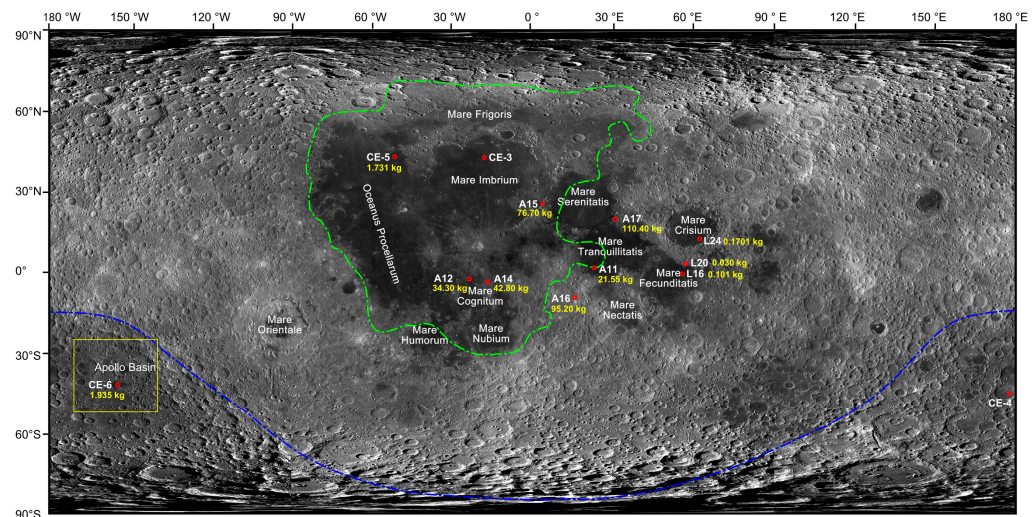


**Figure 1.** Global map showing the landing sites of Apollo (A), Luna (L), and Chang'E (CE) sample return missions. Three major lunar terranes are outlined and shown: the Procellarum KREEP Terrane (PKT, Th > 3.5 ppm) with a green curve and the South Pole–Aitken Terrane (SPA) with a blue curve. The landing sites of the Apollo, Luna, and CE missions are marked as open red circles and the weights of the returned samples are shown with yellow numbers. The yellow rectangle indicates the study area. The lunar sample data are from [23,24]. The Lunar Reconnaissance Orbiter (LRO) Wide Angle Camera (WAC) mosaic [25] is used as the base map (100 m/pixel; simple cylindrical projection).

## 2. Data and Methods

The Apollo basin and its adjacent area (25–50°S, 140–170°W) were selected as the survey region (Figures 1 and 2). Multiple remote sensing data sets and sources were employed for regional topography, geomorphology, chemical composition, and crustal thickness analysis. We used the imaging data collected by the Lunar Reconnaissance Orbiter Camera (LROC) Wide Angle Camera (WAC) mosaic (100 m/pixel) for conducting regional geologic context and geomorphologic analyses of the Apollo basin [25]. The digital elevation model (DEM) produced based on the Lunar Orbiter Laser Altimeter (LOLA) data [26] was used for the topography survey.

The TiO<sub>2</sub> content map from LROC WAC (~400 m/pixel) was used for the compositional characterizations of the mare units in the Apollo basin [27]. The FeO and Th elemental abundance maps obtained by the Lunar Prospector Gamma Ray Spectrometer (LP-GRS) were used for analyzing the chemical compositions of the Apollo basin and its adjacent area. The half-degree FeO abundance map (~15 km/pixel) was acquired during the low altitude observations of LP-GRS. The FeO and Th data sets were firstly produced by [28] and then further calibrated by [29]. The half-degree Th data described by [30] have been used to investigate small-area Th distribution features on the Moon.

The global map of lunar crustal thickness was derived from gravity data obtained by NASA's GRAIL spacecraft [31]. Wicczorek et al. (2013) developed four types of models to calculate lunar crustal thickness with different assumption parameters, for example, density contrasts and average crustal thickness. To determine the crust–mantle boundary of the Apollo basin, a lunar crustal thickness map based on Model 1 [32] with a crustal porosity of 12% and mantle density of 3220 kg/m<sup>3</sup> using gravity model GL0420A truncated beyond degree 310 was adopted in the present study. The model is widely used to evaluate the effect of the crustal structure on magma eruption because it neglects the contribution of mare basaltic layers and the relatively larger porosity is suitable for a study area that is very heavily impacted.

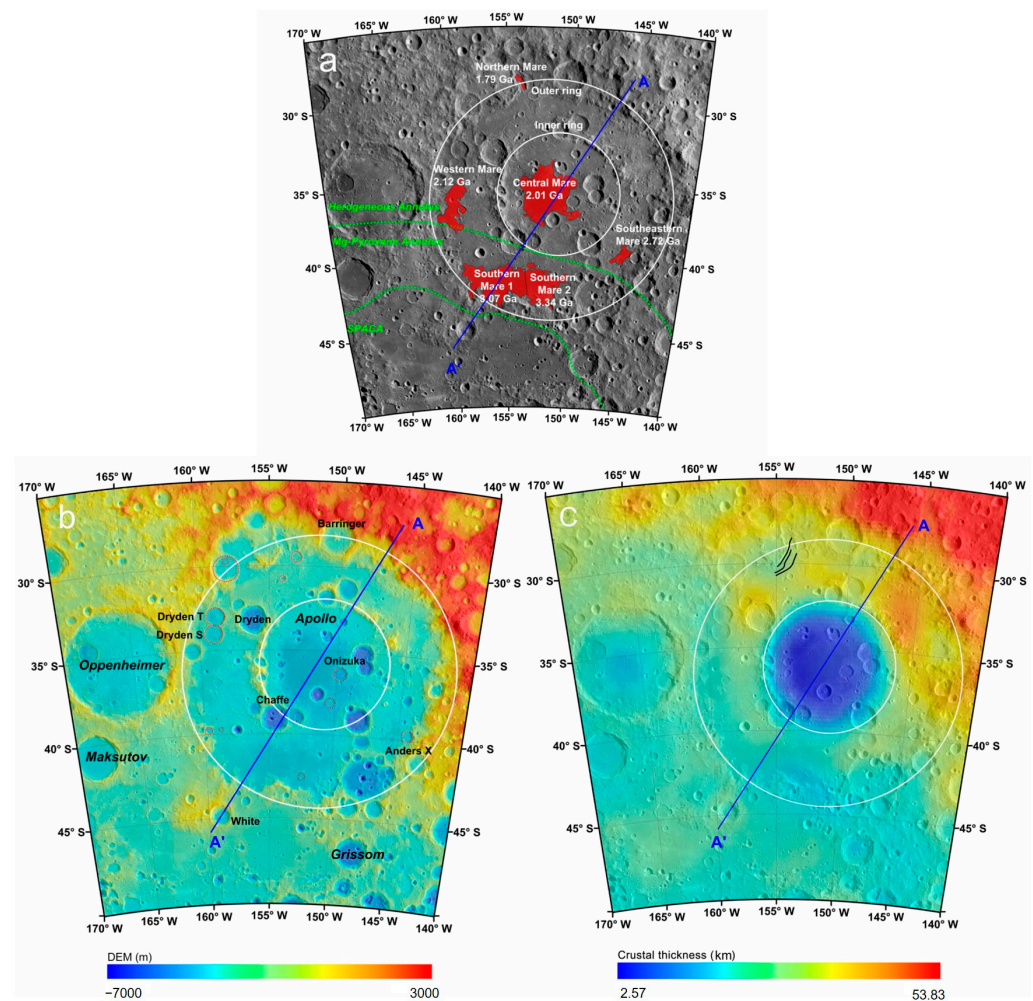


**Figure 2.** Geological contexts of the Apollo basin. (a) LROC WAC mosaic of the Apollo basin showing the rings (the white solid circles) and mare deposits (the red polygons). The green dashed lines are the boundaries of the South Pole–Aitken Compositional Anomaly (SPACA), Mg-pyroxene annulus and heterogeneous annulus. The blue solid lines from A to A' show the position of the crossing profiles. (b) LOLA DEM 100 m/pixel data [26] overlaid on LROC WAC mosaic showing the local topography. The impact basins and craters in the study area are annotated. The red dash circles indicate the floor-fractured craters within the Apollo basin. (c) Crustal thickness of the Apollo basin [32] was overlain on an LRO WAC image. The black curves present graben in the Apollo basin.

### 3. Lateral Heterogeneity of Apollo Basin

#### 3.1. Topography

The Apollo basin is a typical impact basin with well-preserved double rings (Figure 2), although it has been dated as a pre-Nectarian impact structure ( $3.91 \pm 0.04 / -0.06$  Ga [33];  $3.98 \pm 0.04 / -0.06$  Ga [19];  $4.14 \pm 0.024 / -0.029$  Ga [34]). Apollo is also one of the largest impact basins within the SPA. From the LOLA DEM map, the distinctive divide in elevation between the Apollo basin's northeastern and southwestern sections can be noted (Figure 2b). We estimated that the northeastern ridge was generally 4.1 km higher than the southwestern one (Figure 3). The absolute height of the basin floor was about  $-5.0$  km. The partially preserved inner ring was about 3.0 km high above the bottom of the Apollo basin. The clear topographic variations can be explained by its unique location. The Apollo basin sits on the inner northeastern slope of the SPA, a transitional zone from the SPA rim to the SPA floor (Figure 2a). Meanwhile, the Apollo basin crosses the Mg-pyroxene annulus (MPA) and heterogeneous annulus (HA) [35]. The latter exhibits an elevated Mg-rich

pyroxene abundance and has been considered to represent the pyroxene-rich areas mixed with feldspathic materials derived from an essentially anorthositic lunar crust.

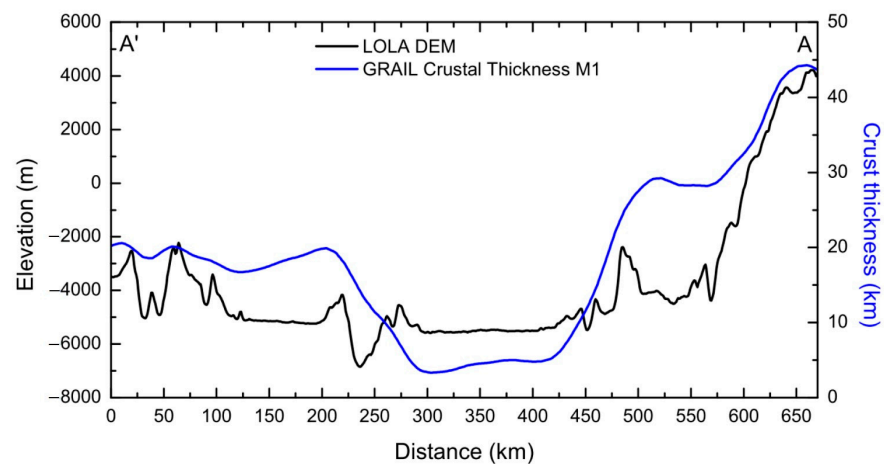


**Figure 3.** The topography (black curve) and crustal thickness (blue curve) profiles crossing the Apollo basin from southwest A' to northeast A (Figure 2).

### 3.2. Mare Volcanism

Large mare deposits cover the central, southern, and western portions of the Apollo basin floor [21]. Two small mare patches (<500 km<sup>2</sup>) were found in the southeastern and northern rim of the basin. Floor-fractured craters (FFCs) and other volcanic features (like grabens and volcanic domes) were identified as well (Figure 2b). All of these indicate the active mare volcanism occurring in the geological history of the study region. Previous studies have investigated the duration, compositions, and volumes of mare basalts in the Apollo basin [20–22,36]. Here, we reviewed these studies and further reveal the lateral heterogeneity of mare volcanism in the Apollo basin.

Firstly, mare deposits are spatially unevenly distributed in the Apollo basin (Figure 2a). Three large areas of mare deposits filled the center of the Apollo basin and its southern and western portions between two rings. In contrast, similar volcanic deposits and associated volcanic features were almost absent in the northeastern part of the Apollo basin floor. Only two isolated volcanic deposits (northwestern and southeastern mare) have been found (Figure 2a). Previous studies have estimated the thickness of mare basalt layers and calculated the volumes of three large mare deposits [22,37]. But even the comparison of mare unit areas demonstrated the obvious difference in mare fluxes. The areas of central, southern, and western mare units are one order larger than those of the southeastern and northwestern mare units (Table 1). The lateral variation in mare volcanism in the Apollo basin indicates that the genesis and emplacement of mare basalts depends on the heterogeneity nature of this region, which will be further discussed in the following sections.

Secondly, the absolute model ages (AMAs) of mare basalts in the Apollo basin ranging from the late Imbrian to Eratosthenian period indicates a long-lasting farside volcanism [20,21,36]. The Southern Mare 2 unit represents the late Imbrian-aged volcanic activity at 3.34 Ga [21]. The following one is the Southern Mare 1 unit which erupted in the early Eratosthenian period and superposed on the western portion of the Imbrian-aged Southern Mare 2 basalt layer. Then, mare basalt emplacement was reactive at 2.14 Ga [21], which produced a flat volcanic plain in the western mare between two rings. The peak of volcanic activity in the Apollo basin occurred around 2.01 Ga, during which mare basalts completely filled its floor center. After this voluminous effusion, mare emplacements in the Apollo basin tended to cease. Only a localized volcanic event at ~1.79 Ga (northern mare) occurred in the northern rims. Here, we summarized the characteristics of mare volcanic activities in the Apollo basin on a global scale: (1) compared with other impact basins (like Imbrium and Orientale), mare volcanism in the Apollo basin started very late (~3.4 Ga);

(2) the peak of volcanic activity in the Apollo basin ( $\sim 2.01$  Ga) postdates global peak of mare activity at 3.2–3.8 Ga; and (3) the young mare basalts (less than 2.0 Ga) are more frequently exposed in the Apollo basin than in the PKT with enhanced concentrations of heat-producing elements such as Th. Possible thermal mechanisms to support such young eruptions have been discussed later.

Thirdly, the mare basalts in the Apollo basin exhibit a large variation of  $\text{TiO}_2$  abundances from 2.0 to 9.65 wt% (Figure 4b). From the image of these mare units, remarkable high albedo ejecta were only found in the central mare. These regions were excluded when determining the average  $\text{TiO}_2$  concentrations of this unit. Using the LROC NAC  $\text{TiO}_2$  data [15], previous study systematically compared the  $\text{TiO}_2$  variations of 17 major maria on the Moon. The  $\text{TiO}_2$  variations in mare basalts in the Apollo basin are comparable with those of Mare Imbrium, although the total mare area within the Apollo basin ( $2.05 \times 10^4 \text{ km}^2$ ) is far less than that of Mare Imbrium ( $1.30 \times 10^5 \text{ km}^2$ ) [38]. The obvious compositional difference in mare basalts in the Apollo basin strongly indicates the heterogeneity nature of mantle source regions. Furthermore, high-Ti and low-Ti mare basalts seem to be emplaced in an alternating sequence. This is also different with the global age- $\text{TiO}_2$  abundance trend that mare basalts with higher  $\text{TiO}_2$  contents show younger ages and low  $\text{TiO}_2$  mare basalts have older ages [39–41].

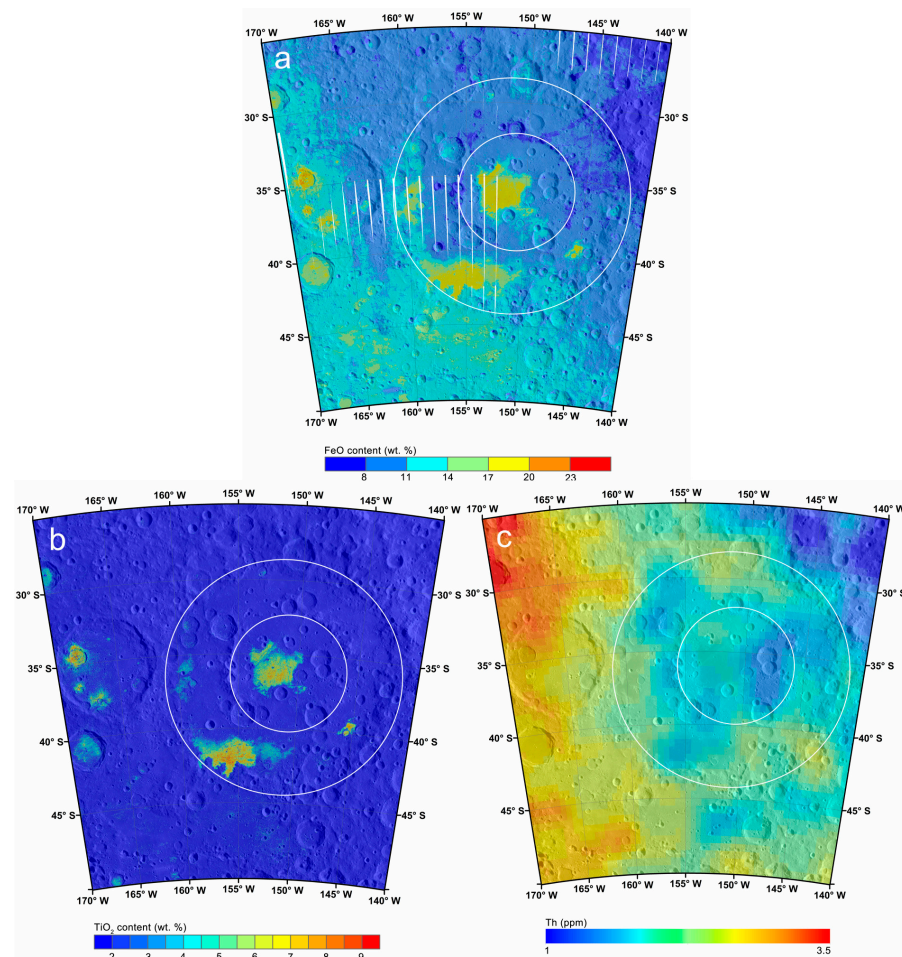


**Figure 4.** Chemical compositions of the Apollo basin. (a) FeO map using Kaguya Multiband Imager (MI) data. (b)  $\text{TiO}_2$  map derived from LROC WAC data. (c) Th map derived from LP-GRS data. The white solid circles represent the Apollo basin rings.

**Table 1.** Comparison of AMAs and chemical compositions of mare units in Apollo basin.

Mare Units	Total Area	Estimated Thickness	Absolute Model Age (Ga)			Average FeO	Average TiO <sub>2</sub>	Average Th	
	(km <sup>2</sup> )	(m)				(wt%)	(wt%)	(ppm)	
Central Mare	8007	260–340	2.01 <sup>+0.10</sup> <sub>−0.10</sub>	2.93 <sup>+0.07</sup> <sub>−0.07</sub>		19.0 ± 0.6	6.5 ± 1.0	1.10	
Western Mare	2501	200–340	2.12 <sup>+0.14</sup> <sub>−0.14</sub>	3.39 <sup>+0.02</sup> <sub>−0.02</sub>		16.7 ± 0.6	3.2 ± 0.6	1.45	
Southern Mare 1	5760	170–350	3.07 <sup>+0.07</sup> <sub>−0.08</sub>	2.40 <sup>+0.11</sup> <sub>−0.11</sub>	3.31 <sup>+0.02</sup> <sub>−0.02</sub>	2.50 <sup>+0.078</sup> <sub>−0.080</sub>	18.3 ± 0.7	6.2 ± 1.0	1.34
Southern Mare 2	3569		3.34 <sup>+0.04</sup> <sub>−0.06</sub>	3.43 <sup>+0.04</sup> <sub>−0.06</sub>	3.45 <sup>+0.04</sup> <sub>−0.05</sub>		16.6 ± 1.0	3.2 ± 0.5	
Northern Mare	176		1.79 <sup>+0.26</sup> <sub>−0.26</sub>	2.40 <sup>+0.31</sup> <sub>−0.32</sub>		13.1 ± 0.8	2.2 ± 0.5		
Southeastern Mare	457		2.72 <sup>+0.20</sup> <sub>−0.24</sub>	3.38 <sup>+0.05</sup> <sub>−0.07</sub>		18.0 ± 0.6	6.2 ± 0.9		
References	[21]	[22]	[21]	[36]	[20]	[42]	[21]	[21]	This study

### 3.3. Iron and Th Abundance

Iron and thorium are useful for understanding the chemical composition and petrogenetic interpretation of the lunar surface. The FeO and Th abundances have been well measured by LP-GRS over the entire lunar surface [28,30]. Wieczorek and Phillips (2000) proposed that Th and other heat-produced elements concentrated in the lower crust of the PKT region could result in partial melting in the underlying mantle after crystallization of the LMO [43]. This has been used to explain the occurrence of young mare basalts in Ocean Procellarum and Mare Imbrium.

However, the Apollo basin including mare basalt within it is characterized by low Th abundance (Figure 4c). The Apollo floor and peak ring as well as mare basalts are all lower than 2.0 ppm. And the variations in Th abundance among them are quite subtle. Th abundances of the central mare, western mare, and southern mare are 1.11, 1.45, and 1.34 ppm, respectively. Hagerty et al. (2011) obtained a high-resolution Th map of mare regions in the SPA using the forward modeling of the LP GRS Th data [44]. Their results revealed that all the three large mare units in the Apollo basin contain little or no Th, which has been further confirmed by the Kaguya GRS data [45]. The depletion of Th in the Apollo basin seems to be contradicted by the presence of abundant young mare basalt within it. Therefore, we could rule out heat-producing elements as a thermal source for mare volcanism in the Apollo basin.

### 3.4. Crustal Thickness

According to mare basalt ascent and eruption models, mantle-derived magmas could have been extruded to the surface preferentially with the thin anorthositic crust [4,7,46,47] because basaltic magmas are denser than that of lunar crust. Therefore, the paucity of lunar farside mare basalt can be explained. The basaltic magmas cannot reach the surface due to the thick crust of the lunar farside; large impact basins with thin crusts are the exception. The height to which lavas can rise depends on the density difference between the basaltic magma and that of the overlying lunar crustal rocks.

The Apollo basin straddles the northeastern rims and interior of the SPA basin, which results in the crustal thickness asymmetry within the Apollo basin. Here, the crustal thickness derived from the GRAIL mission [32] was used to reveal lateral crustal thickness variations in the Apollo basin (Figure 2c and Figure 3). The thicker crust was present on the northeastern section of the basin (>45 km). The annulus region between the Apollo's inner and outer rings had a relatively thinner crust ranging from 18 to 30 km, and the crustal thickness notably decreased along the northeastern to southeastern directions (Figure 3). The central portion of the basin exhibited the thinnest crust (3–5 km), making it one of the thinnest crustal locations on the Moon.

## 4. Discussion

### 4.1. Taking the Apollo Basin as an Example to Evaluate Mare Basalt Genesis Models

The sources of the mare basalts which filled the lunar large basins have historically been the subject of much debate, although it is generally accepted that they should originate from partial melting of the lunar magma ocean cumulates. However, the returned mare basalts and basaltic meteorite as well as remote surveys have revealed the wide variety of the ages, compositions, source depths, and tectonic environment of mare volcanism [7]. Several mare basalt genesis models have been proposed to explain mare volcanism occurring on the different regions on the Moon [48]. Coupled with mare volcanism within the Apollo basin, these five models were briefly reviewed and evaluated.

Model 1: The asymmetrical distribution of mare basalts on the lunar nearside and farside has long been noted. Lunar crustal thickness has been considered to be responsible for this global asymmetry of mare basalt [5,7], as the thinner crust favored mare basalt formation and magma ascent. The distribution of mare basalts and its dependence on crustal thickness have been noted on a global scale, especially within the lunar nearside. However, the SPA is not extensively emplaced by mare basalts as expected, although the SPA is the largest basin with a relatively thinner crust on a global scale [20].

In the above section, we have demonstrated the lateral variations in crustal thickness within the Apollo basin. Four large mare units (central mare, western mare, and southern mare 1 and 2) all occur in the regions with a crustal thickness <30 km. The asymmetric distribution of mare deposits in the Apollo basin is strongly correlated with local crustal thickness. In addition, the floor-fractured craters (FFCs) identified in the Apollo basin are all located to the southwest half of this basin [21]. Therefore, the thinner crust favors the mare basalt genesis, and then the basaltic magma can ascend by dike propagation ascent in the Apollo basin. This model is also prevalent in mare volcanisms of other large impact basins like Orientale [48].

Model 2: Impact events in the early history of the Moon produced impact basins. Most of them are filled with large volumes of mare basalt. These observations support a potential link between impacts and volcanism. Hydrodynamic modeling demonstrated that large impacts (~200 km diameter crater) can remove significant massive material from the impact site, and the subsequent uplifts underlying mantle materials could lead to decompression melting (or pressure release melting). This in situ process could cause a long-lived volcanism within a large basin [49]. Elkins-Tanton and Hager (2005) further argued the viability of decompression melting and proposed a two-stage model for magma generation [50]. The crater excavation firstly results in immediate in situ decompression and is followed by a long-lasting mantle convective process [50]. Their model predicts that an impact event generating a 600 km diameter crater in 75 km lithosphere could produce  $10^6 \text{ km}^3$  mafic magmas, being comparable with individual terrestrial flood-basalt provinces.

As motioned above, the Apollo basin is dated as a pre-Nectarian impact structure (3.91–4.14 Ga, [19,33,34]). However, several craters counting for mare units within the Apollo basin all suggest that the mare basalts in this basin should not be emplaced until 3.34 Ga (Table 1). This obvious time gap shows that the Apollo basin formation and mare volcanism within it were not instantaneous. Therefore, mare basalts in the Apollo basin should not be products of decompression melting. Despite this, the SPA and Apollo impacts both excavated a substantial portion of the crust at the region, which leads to substantial mantle uplift [51]. Although the impact event may not have directly triggered lava floods in the Apollo basin, the event still created favorable conditions for subsequent volcanic eruptions.

Model 3: The PKT outlined by Jolliff et al. (2000) exhibits a prolonged mare basalt volcanism from at least ~4.1 to ~1.2 Ga [11,40]. Meanwhile, the terrane is geochemically characterized by the enrichment of radioactive heat-producing elements (Th, U, and K) and other incompatible elements [52]. It has been proposed that the KREEP layer exists between the lunar crust and mantle and significantly affects the thermal evolution of the PKT. The heat released by radioactive Th, U, and K elements can maintain the mantle below the

PKT partially molten. This model explains the abundant mare flooding, a long-lived lunar volcanism, and the occurrence of “red spot” or non-mare volcanism within the PKT region.

The Apollo basin maintains prolonged volcanic activity from 3.34 to 1.79 Ga. The northern mare (1.79 Ga) of the Apollo basin is even younger than the CE-5 mare basalt (2.0 Ga) [53,54] and many Eratosthenian-aged mare units in the PKT [11,40]. However, the Apollo basin and its vicinity does not show any enhanced concentrations of Th (<2.0 ppm LP GRS) or other heat-producing elements. The characteristic “red spot” volcanic structures are also absent in the Apollo basin. Therefore, the KREEP-induced melting cannot explain mare volcanism of the Apollo basin. These observations also indicate that the Apollo basin should have a thermal history distinct from the lunar nearside. Without radiogenic heating, there must be another heat source or an insulating layer (that can prevent the interior from fast cooling) to maintain a partial melt zone in the Moon [55].

Model 4: Lunar samples collected by Apollo 11 missions first led to the lunar magma ocean (LMO) hypothesis. It argued that the crystallization of the global magma ocean produced the anorthositic crust and mafic cumulate interior. Dense, ilmenite-bearing cumulate (IBC) with elevated incompatible radioactive elements formed during the late stage of lunar magma ocean beneath the crust, which is denser than the underlying earlier mafic cumulates [56–62]. Due to the gravitational instabilities, the dense cumulates would sink deep into the mantle bottom [59], so-called the lunar mantle overturn. After this, the radioactive elements within the IBC could heat the overlying mantle and produce partial melting. The large-scale overturn process has a profound influence on subsequent lunar magmatic episodes (i.e., age, composition, and spatial distribution of magmatism).

In the above section, we have summarized that (1) the mare basalts in the Apollo basin exhibit a large variation of  $\text{TiO}_2$  abundances, and (2) high-Ti and low-Ti mare basalts seem to be emplaced in an alternating sequence. The compositional diversity of lunar mare basalts in the Apollo basin should be a consequence of the lunar mantle overturn after the LMO solidification. The overturn between the top IBC layer and underlying mafic cumulates will not have been completely efficient, leaving a significant proportion of IBC within the depth range of the origin of mare magmas [63]. This may explain the alternating emplacement of high-Ti and low-Ti mare basalts of the Apollo basin.

Model 5: Mare volcanism in lunar large basins typically postdate the basin-forming impact events. Therefore, this model emphasizes the influence of global thermal evolution and basin evolution on mare volcanism after the formation of impact basin. The evolving global state of stress in the lithosphere and the increased loading of mare basalts in impact basins controls the location of eruptive vents, the style of emplacement, and the extrusive volumes of mare basalts [46,64,65].

According to this model’s predictions, early mare volcanism will concentrate in the basin center while the young mare deposits will present on the edges of the basin [48] because extensional stresses within a basin are supposed to move radially outward over time. Mare volcanism with the Orientale basin generally follows this trend. In contrast, the Apollo basin does not support the idea: the central mare unit is clearly younger than all the three large mare units occurring between two rings (Table 1). This suggests that postbasin loading and stress fields of the Apollo basin may be different from the model’s predictions. It has also been noted that three large mare flows are located along the outer ring of the Apollo basin, except for the central mare. The alternative explanation is that the normal faults occurring along outer ring cut through the local crust and extend down into the mantle, and these ring faults act as conduits for magma ascent (Figure 5).

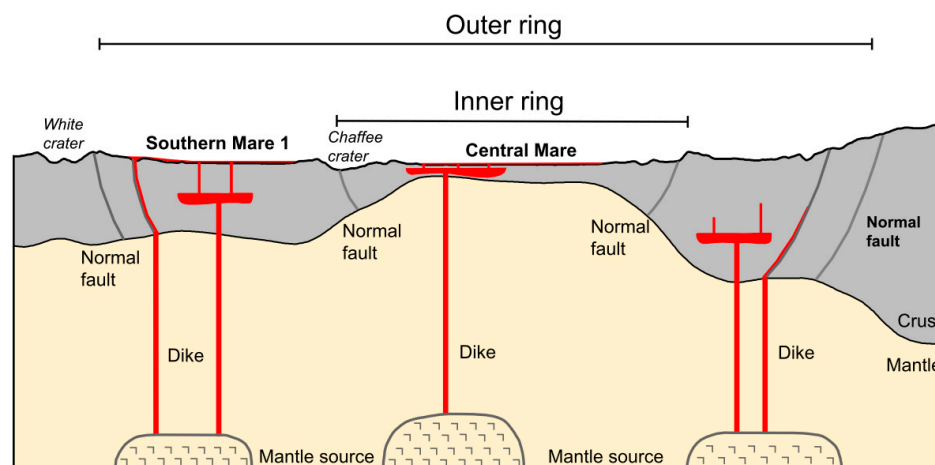


**Figure 5.** Sketch maps for mare volcanism in the Apollo basin. The subsurface structure of the Apollo basin along the profile is shown in Figure 2 from southwest A' to northeast A. The depth is not scaled in the profile. We predicted the concentric normal faults occurring along the impact basin rings. The thin crust offers an extensional tectonic background for magma ascent as well, especially for the central mare.

#### 4.2. Implications for Laboratory Investigations of Chang'E-6 Mare Basalt Samples

The CE-6 spacecraft successfully returned a total of 1935.3 g of lunar soil samples from the Southern Mare 1 unit. Local mare basalt of the landing site was of the high-Ti type (6.2 wt%) with an absolute model age of 3.07 Ga [21]. As the first mare basalt sample from the lunar farside, CE-6 mare basalts expand the diversity of existing collected samples. Laboratory investigations will determine the mineralogy and geochemistry of CE-6 mare basalts. These results could reveal the petrogenesis of the lunar farside mare basalt, constrain the geochemistry and depths of mare basalt sources, explore lunar interior heterogeneity, and further evaluate the timing and scale of the lunar mantle overturn. The radioisotopic dating of CE-6 mare basalts will provide accurate ages for lunar farside volcanism, which is crucial for understanding the thermal evolution of the Moon. Meanwhile, the CE-6 chronology data will build the first calibration point on the lunar farside. This will greatly improve the lunar cratering chronology models [36].

Volcanism and impact cratering are the primary geologic processes that shaped the Moon. The link between mare volcanism and impact basin formation/evolution infers to number of unresolved questions [7]. The Apollo is a typical peak-ring impact basin; CE-6 soil represents the samples of mare lavas that have flooded and filled the Apollo basin. Based on the above remote survey, we concluded that the generation of mare basalt magmas and their emplacement in the Apollo basin seems strongly related to lunar crustal thickness, and the composition diversity of mare basalt may reflect the heterogeneity of mantle sources. The heterogeneous mantle could be related to (1) the solidification of a global magma ocean and subsequent mantle overturn and (2) the large impact-induced mantle convection and migration beneath the SPA basin [66]. Despite this, many outstanding questions about mare volcanism in the Apollo basin still exist, including (1) what supports a prolonged mare volcanism in this basin and what does this reflect an unique thermal history of this region; (2) why the central mare is younger than other mare units, and what is the relationship of mare basalt emplacement and tectonic backgrounds (postbasin loading, stress fields and ring faults); and (3) what is the chemical nature of mare basalts of the Apollo basin, and the differences in comparison with mare basalts collected from lunar nearside, and how the SPA formation event influences their mantle sources. Therefore, the CE-6 mare basalt offers an opportunity to unravel the mare volcanic history of the lunar farside and the connections between the mare volcanism and impact basin formation/evolution.

## 5. Conclusions

Using remote sensing data, we found that the Apollo basin exhibits an overall asymmetric configuration in the distribution of mare basalts as well as its topography, chemical compositions, and crustal thickness. As a large impact structure on the lunar farside, the Apollo basin is an excellent example of evaluating the proposed mare basalt genesis models on a global scale.

The generation of mare basalt magmas and their emplacement in the Apollo basin seems to be strongly related with local crustal thickness (<30 km). However, the formation of basaltic magmas should be independent to the decompression melting because the mare units (3.34–1.79 Ga) are much younger than the pre-Nectarian Apollo basin. The mare basalts filled in the Apollo basin exhibit a large variation of TiO<sub>2</sub> content indicating the heterogeneity of mantle sources, which is possibly due to the lunar mantle overturn after the LMO solidification or the impact-induced mantle convection and migration.

The prolonged mare volcanic history of the Apollo basin is not well explained, especially considering the low-Th (<2 ppm) feature of this region. In addition, the central mare erupted later than other mare units within the Apollo basin. This is clearly different from the sequence of mare volcanism in the Orientale basin and also contradicts the predictions of the postbasin loading-induced stresses model.

Laboratory investigations will determine the compositions, ages, and source region depths of the Chang'E-6 mare basalt sample. Laboratory data could possibly answer the above questions and provide new insight into the mare volcanic history of the lunar farside and the connections between mare volcanism and impact basin formation/evolution.

**Author Contributions:** Conceptualization, X.F.; methodology, C.Y. and J.L.; data curation, C.Y., J.L. and S.C.; writing—original draft preparation, X.F.; writing—review and editing, X.F., C.Y., J.L., S.C., J.C., J.Z. and B.L.; funding acquisition, X.F. All authors have read and agreed to the published version of the manuscript.

**Funding:** This work was funded by the National Key Research and Development Program of China (2022YFF0503100), the National Natural Science Foundation of China (42273039), and Pre-research project on Civil Aerospace Technologies by CNAS (Grant No. D020201).

**Data Availability Statement:** All original LROC images are available from NASA's Planetary Data System (<http://pds.nasa.gov/>) (accessed on 7 April 2024), and Kaguya MI mineral maps are available from the Imaging Annex of the Planetary Data System (<http://astrogeology.usgs.gov/pds/annex>) (accessed on 7 April 2024). The GRAIL lunar crustal thickness model data were accessed from <https://zenodo.org/records/997347> (accessed on 7 April 2024). The data for Figure 3 are available in Zenodo at 10.5281/zenodo.13688826 (accessed on 4 August 2024).

**Acknowledgments:** Fu X. H. is also supported by the Tang Scholar of Shandong University and the Young Scholars Program of Shandong University, Weihai.

**Conflicts of Interest:** The authors declare no conflicts of interest.

## References

1. Head, J.W.; Wilson, L.; Hiesinger, H.; van der Bogert, C.; Chen, Y.; Dickson, J.L.; Gaddis, L.R.; Haruyama, J.; Jawin, E.R.; Jozwiak, L.M.; et al. Lunar Mare Basaltic Volcanism: Volcanic Features and Emplacement Processes. *Rev. Mineral. Geochem.* **2023**, *89*, 453–507. [[CrossRef](#)]
2. Whitten, J.; Head, J.W. Lunar cryptomaria: Mineralogy and composition of ancient volcanic deposits. *Planet. Space Sci.* **2015**, *106*, 67–81. [[CrossRef](#)]
3. Head, J.W., III. Lunar volcanism in space and time. *Rev. Geophys.* **1976**, *14*, 265–300. [[CrossRef](#)]
4. Head, J.W.; Wilson, L. Generation, ascent and eruption of magma on the Moon: New insights into source depths, magma supply, intrusions and effusive/explosive eruptions (Part 2: Predicted emplacement processes and observations). *Icarus* **2017**, *283*, 176–223. [[CrossRef](#)]
5. Wilson, L.; Head, J.W., III. Ascent and eruption of basaltic magma on the Earth and Moon. *J. Geophys. Res. Solid Earth* **1981**, *86*, 2971–3001. [[CrossRef](#)]
6. Wilson, L.; Head, J.W. Controls on Lunar Basaltic Volcanic Eruption Structure and Morphology: Gas Release Patterns in Sequential Eruption Phases. *Geophys. Res. Lett.* **2018**, *45*, 5852–5859. [[CrossRef](#)]

7. Head, J.W.; Wilson, L. Lunar mare volcanism: Stratigraphy, eruption conditions, and the evolution of secondary crusts. *Geochim. Cosmochim. Acta* **1992**, *56*, 2155–2175. [[CrossRef](#)]
8. Joy, K.H.; Arai, T. Lunar meteorites: New insights into the geological history of the Moon. *Astron. Geophys.* **2013**, *54*, 4.28–4.32. [[CrossRef](#)]
9. Nyquist, L.E.; Shih, C.Y. The isotopic record of lunar volcanism. *Geochim. Cosmochim. Acta* **1992**, *56*, 2213–2234. [[CrossRef](#)]
10. Hiesinger, H.; Head, J.W., III; Wolf, U.; Jaumann, R.; Neukum, G. Ages and stratigraphy of mare basalts in Oceanus Procellarum, Mare Nubium, Mare Cognitum, and Mare Insularum. *J. Geophys. Res. Planets* **2003**, *108*, 5065. [[CrossRef](#)]
11. Hiesinger, H.; Head, J.W., III; Wolf, U.; Jaumann, R.; Neukum, G. Ages and stratigraphy of lunar mare basalts: A synthesis. In *Recent Advances and Current Research Issues in Lunar Stratigraphy*; Ambrose, W.A., Williams, D.A., Eds.; Geological Society of America: Boulder, CO, USA, 2011.
12. Hallis, L.J.; Anand, M.; Strekopytov, S. Trace-element modelling of mare basalt parental melts: Implications for a heterogeneous lunar mantle. *Geochim. Cosmochim. Acta* **2014**, *134*, 289–316. [[CrossRef](#)]
13. Neal, C.R.; Taylor, L.A. Petrogenesis of mare basalts: A record of lunar volcanism. *Geochim. Cosmochim. Acta* **1992**, *56*, 2177–2211. [[CrossRef](#)]
14. Qian, Y.; She, Z.; He, Q.; Xiao, L.; Wang, Z.; Head, J.W.; Sun, L.; Wang, Y.; Wu, B.; Wu, X.; et al. Mineralogy and chronology of the young mare volcanism in the Procellarum-KREEP-Terrane. *Nat. Astron.* **2023**, *7*, 287–297. [[CrossRef](#)]
15. Sato, H.; Robinson, M.S.; Lawrence, S.J.; Denevi, B.W.; Hapke, B.; Jolliff, B.L.; Hiesinger, H. Lunar mare TiO<sub>2</sub> abundances estimated from UV/Vis reflectance. *Icarus* **2017**, *296*, 216–238. [[CrossRef](#)]
16. Shearer, C.K.; Hess, P.C.; Wieczorek, M.A.; Pritchard, M.E.; Parmentier, E.M.; Borg, L.E.; Longhi, J.; Elkins-Tanton, L.T.; Neal, C.R.; Antonenko, I.; et al. Thermal and Magmatic Evolution of the Moon. *Rev. Mineral. Geochem.* **2006**, *60*, 365–518. [[CrossRef](#)]
17. Potter, R.W.K.; Head, J.W.; Guo, D.; Liu, J.; Xiao, L. The Apollo peak-ring impact basin: Insights into the structure and evolution of the South Pole–Aitken basin. *Icarus* **2018**, *306*, 139–149. [[CrossRef](#)]
18. Wang, X.; Head, J.W.; Qian, Y.; Zhao, W.; Liu, J.; Gao, Y.; Wu, B. Possible Lithological Types and Scientific Significance of the Sample to be Returned by Chang'E-6 Mission. In Proceedings of the 55th Lunar and Planetary Science Conference, The Woodlands, TX, USA, 11–15 March 2024; p. 1873.
19. Ivanov, M.A.; Hiesinger, H.; van der Bogert, C.H.; Orgel, C.; Pasckert, J.H.; Head, J.W. Geologic History of the Northern Portion of the South Pole–Aitken Basin on the Moon. *J. Geophys. Res. Planets* **2018**, *123*, 2585–2612. [[CrossRef](#)]
20. Pasckert, J.H.; Hiesinger, H.; van der Bogert, C.H. Lunar farside volcanism in and around the South Pole–Aitken basin. *Icarus* **2018**, *299*, 538–562. [[CrossRef](#)]
21. Qian, Y.; Head, J.; Michalski, J.; Wang, X.; van der Bogert, C.H.; Hiesinger, H.; Sun, L.; Yang, W.; Xiao, L.; Li, X.; et al. Long-lasting farside volcanism in the Apollo basin: Chang'e-6 landing site. *Earth Planet. Sci. Lett.* **2024**, *637*, 118737. [[CrossRef](#)]
22. Taguchi, M.; Morota, T.; Kato, S. Lateral heterogeneity of lunar volcanic activity according to volumes of mare basalts in the farside basins. *J. Geophys. Res. Planets* **2017**, *122*, 1505–1521. [[CrossRef](#)]
23. Meyer, C. Lunar Sample Compendium. 2009. Available online: <https://ntrs.nasa.gov/api/citations/20090041867/downloads/20090041867.pdf> (accessed on 5 September 2024).
24. Li, C.; Hu, H.; Yang, M.-F.; Pei, Z.-Y.; Zhou, Q.; Ren, X.; Liu, B.; Liu, D.; Zeng, X.; Zhang, G.; et al. Characteristics of the lunar samples returned by the Chang'E-5 mission. *Natl. Sci. Rev.* **2021**, *9*, nwab188. [[CrossRef](#)] [[PubMed](#)]
25. Robinson, M.S.; Brylow, S.M.; Tschimmel, M.; Humm, D.; Lawrence, S.J.; Thomas, P.C.; Denevi, B.W.; Bowman-Cisneros, E.; Zerr, J.; Ravine, M.A.; et al. Lunar Reconnaissance Orbiter Camera (LROC) Instrument Overview. *Space Sci. Rev.* **2010**, *150*, 81–124. [[CrossRef](#)]
26. Smith, D.E.; Zuber, M.T.; Jackson, G.B.; Cavanaugh, J.F.; Neumann, G.A.; Riris, H.; Sun, X.; Zellar, R.S.; Coltharp, C.; Connelly, J.; et al. The Lunar Orbiter Laser Altimeter Investigation on the Lunar Reconnaissance Orbiter Mission. *Space Sci. Rev.* **2010**, *150*, 209–241. [[CrossRef](#)]
27. Sato, H.; Hapke, B.; Robinson, M.S. New Extended Range WAC TiO<sub>2</sub> Map of the Moon. In Proceedings of the 52nd Lunar and Planetary Science Conference, The Woodlands, TX, USA, 15–19 March 2021; p. 1031.
28. Lawrence, D.J.; Feldman, W.C.; Elphic, R.C.; Little, R.C.; Prettyman, T.H.; Maurice, S.; Lucey, P.G.; Binder, A.B. Iron abundances on the lunar surface as measured by the Lunar Prospector gamma-ray and neutron spectrometers. *J. Geophys. Res. Planets* **2002**, *107*, 5130. [[CrossRef](#)]
29. Prettyman, T.H.; Hagerty, J.J.; Elphic, R.C.; Feldman, W.C.; Lawrence, D.J.; McKinney, G.W.; Vaniman, D.T. Elemental composition of the lunar surface: Analysis of gamma ray spectroscopy data from Lunar Prospector. *J. Geophys. Res. Planets* **2006**, *111*, E12007. [[CrossRef](#)]
30. Lawrence, D.J.; Elphic, R.C.; Feldman, W.C.; Prettyman, T.H.; Gasnault, O.; Maurice, S. Small-area thorium features on the lunar surface. *J. Geophys. Res. Planets* **2003**, *108*, 5102. [[CrossRef](#)]
31. Zuber, M.T.; Smith, D.E.; Watkins, M.M.; Asmar, S.W.; Konopliv, A.S.; Lemoine, F.G.; Melosh, H.J.; Neumann, G.A.; Phillips, R.J.; Solomon, S.C.; et al. Gravity Field of the Moon from the Gravity Recovery and Interior Laboratory (GRAIL) Mission. *Science* **2013**, *339*, 668–671. [[CrossRef](#)]
32. Wieczorek, M.A.; Neumann, G.A.; Nimmo, F.; Kiefer, W.S.; Taylor, G.J.; Melosh, H.J.; Phillips, R.J.; Solomon, S.C.; Andrews-Hanna, J.C.; Asmar, S.W.; et al. The Crust of the Moon as Seen by GRAIL. *Science* **2013**, *339*, 671–675. [[CrossRef](#)]

33. Hiesinger, H.; van der Bogert, C.H.; Pasckert, J.H.; Schmedemann, N.; Robinson, M.S.; Jolliff, B.; Petro, N. New Crater Size-Frequency Distribution Measurements of the South Pole-Aitken Basin. In Proceedings of the 43rd Annual Lunar and Planetary Science Conference, The Woodlands, TX, USA, 19–23 March 2012; p. 2863.
34. Orgel, C.; Michael, G.; Fassett, C.I.; van der Bogert, C.H.; Riedel, C.; Kneissl, T.; Hiesinger, H. Ancient Bombardment of the Inner Solar System: Reinvestigation of the “Fingerprints” of Different Impactor Populations on the Lunar Surface. *J. Geophys. Res. Planets* **2018**, *123*, 748–762. [[CrossRef](#)]
35. Moriarty III, D.P.; Pieters, C.M. The Character of South Pole-Aitken Basin: Patterns of Surface and Subsurface Composition. *J. Geophys. Res. Planets* **2018**, *123*, 729–747. [[CrossRef](#)]
36. Zeng, X.; Liu, D.; Chen, Y.; Zhou, Q.; Ren, X.; Zhang, Z.; Yan, W.; Chen, W.; Wang, Q.; Deng, X.; et al. Landing site of the Chang’e-6 lunar farside sample return mission from the Apollo basin. *Nat. Astron.* **2023**, *7*, 1188–1197. [[CrossRef](#)]
37. Yingst, R.A.; Head, J.W., III. Volumes of lunar lava ponds in South Pole-Aitken and Orientale Basins: Implications for eruption conditions, transport mechanisms, and magma source regions. *J. Geophys. Res. Planets* **1997**, *102*, 10909–10931. [[CrossRef](#)]
38. Hiesinger, H.; Jaumann, R.; Neukum, G.; Head, J.W., III. Ages of mare basalts on the lunar nearside. *J. Geophys. Res. Planets* **2000**, *105*, 29239–29275. [[CrossRef](#)]
39. Kodama, S.; Yamaguchi, Y. Mare Volcanism on the Moon Inferred from Clementine UVVIS Data. In Proceedings of the 36th Annual Lunar and Planetary Science Conference, League City, TX, USA, 14–18 March 2005; p. 1641.
40. Morota, T.; Haruyama, J.; Ohtake, M.; Matsunaga, T.; Honda, C.; Yokota, Y.; Kimura, J.; Ogawa, Y.; Hirata, N.; Demura, H.; et al. Timing and characteristics of the latest mare eruption on the Moon. *Earth Planet. Sci. Lett.* **2011**, *302*, 255–266. [[CrossRef](#)]
41. Pieters, C.M.; Head, J.W.; Adams, J.B.; McCord, T.B.; Zisk, S.H.; Whitford-Stark, J.L. Late high-titanium basalts of the Western Maria: Geology of the Flamsteed REgion of Oceanus Procellarum. *J. Geophys. Res. Solid Earth* **1980**, *85*, 3913–3938. [[CrossRef](#)]
42. Yue, Z.; Gou, S.; Sun, S.; Yang, W.; Chen, Y.; Wang, Y.; Lin, H.; Di, K.; Lin, Y.; Li, X.; et al. Geological context of the Chang’e-6 landing area and implications for sample analysis. *Innov.* **2024**, *5*, 100663. [[CrossRef](#)]
43. Wieczorek, M.A.; Phillips, R.J. The “Procellarum KREEP Terrane”: Implications for mare volcanism and lunar evolution. *J. Geophys. Res. Planets* **2000**, *105*, 20417–20430. [[CrossRef](#)]
44. Hagerty, J.J.; Lawrence, D.J.; Hawke, B.R. Thorium abundances of basalt ponds in South Pole-Aitken basin: Insights into the composition and evolution of the far side lunar mantle. *J. Geophys. Res. Planets* **2011**, *116*. [[CrossRef](#)]
45. Naito, M.; Hasebe, N.; Nagaoka, H.; Wöhler, C.; Berezhnoy, A.A.; Bhatt, M.; Kim, K.J. Potassium and Thorium Abundances at the South Pole-Aitken Basin Obtained by the Kaguya Gamma-Ray Spectrometer. *J. Geophys. Res. Planets* **2019**, *124*, 2347–2358. [[CrossRef](#)]
46. Solomon, S.C. Mare Volcanism and Lunar Crustal Structure. In Proceedings of the Lunar and Planetary Science Conference, Houston, TX, USA, 17–21 March 1975; p. 762.
47. Wieczorek, M.A.; Zuber, M.T.; Phillips, R.J. The role of magma buoyancy on the eruption of lunar basalts. *Earth Planet. Sci. Lett.* **2001**, *185*, 71–83. [[CrossRef](#)]
48. Whitten, J.; Head, J.W.; Staid, M.; Pieters, C.M.; Mustard, J.; Clark, R.; Nettles, J.; Klima, R.L.; Taylor, L. Lunar mare deposits associated with the Orientale impact basin: New insights into mineralogy, history, mode of emplacement, and relation to Orientale Basin evolution from Moon Mineralogy Mapper (M3) data from Chandrayaan-1. *J. Geophys. Res. Planets* **2011**, *116*, E00G09. [[CrossRef](#)]
49. Jones, A.P.; Price, G.D.; Price, N.J.; DeCarli, P.S.; Clegg, R.A. Impact induced melting and the development of large igneous provinces. *Earth Planet. Sci. Lett.* **2002**, *202*, 551–561. [[CrossRef](#)]
50. Elkins-Tanton, L.T.; Hager, B.H. Giant meteoroid impacts can cause volcanism. *Earth Planet. Sci. Lett.* **2005**, *239*, 219–232. [[CrossRef](#)]
51. Guo, D.; Bao, Y.; Liu, Y.; Wu, X.; Xu, Y.; Yang, Y.; Zhang, F.; Jolliff, B.; Li, S.; Zhao, Z.; et al. Geological investigation of the lunar Apollo basin: From surface composition to interior structure. *Earth Planet. Sci. Lett.* **2024**, *646*, 118986. [[CrossRef](#)]
52. Jolliff, B.L.; Gillis, J.J.; Haskin, L.A.; Korotev, R.L.; Wieczorek, M.A. Major lunar crustal terranes: Surface expressions and crust-mantle origins. *J. Geophys. Res. Planets* **2000**, *105*, 4197–4216. [[CrossRef](#)]
53. Che, X.; Nemchin, A.; Liu, D.; Long, T.; Wang, C.; Norman, M.D.; Joy, K.H.; Tartese, R.; Head, J.; Jolliff, B.; et al. Age and composition of young basalts on the Moon, measured from samples returned by Chang’e-5. *Science* **2021**, *374*, 887–890. [[CrossRef](#)]
54. Li, Q.-L.; Zhou, Q.; Liu, Y.; Xiao, Z.; Lin, Y.; Li, J.-H.; Ma, H.-X.; Tang, G.-Q.; Guo, S.; Tang, X.; et al. Two-billion-year-old volcanism on the Moon from Chang’e-5 basalts. *Nature* **2021**, *600*, 54–58. [[CrossRef](#)]
55. Ziethe, R.; Seiferlin, K.; Hiesinger, H. Duration and extent of lunar volcanism: Comparison of 3D convection models to mare basalt ages. *Planet. Space Sci.* **2009**, *57*, 784–796. [[CrossRef](#)]
56. Charlier, B.; Grove, T.L.; Namur, O.; Holtz, F. Crystallization of the lunar magma ocean and the primordial mantle-crust differentiation of the Moon. *Geochim. Cosmochim. Acta* **2018**, *234*, 50–69. [[CrossRef](#)]
57. Elkins-Tanton, L.T.; Burgess, S.; Yin, Q.-Z. The lunar magma ocean: Reconciling the solidification process with lunar petrology and geochronology. *Earth Planet. Sci. Lett.* **2011**, *304*, 326–336. [[CrossRef](#)]
58. Haupt, C.P.; Renggli, C.J.; Rohrbach, A.; Berndt, J.; Klemme, S. Experimental Constraints on the Origin of the Lunar High-Ti Basalts. *J. Geophys. Res. Planets* **2024**, *129*, e2023JE008239. [[CrossRef](#)]
59. Hess, P.C.; Parmentier, E.M. A model for the thermal and chemical evolution of the Moon’s interior: Implications for the onset of mare volcanism. *Earth Planet. Sci. Lett.* **1995**, *134*, 501–514. [[CrossRef](#)]

60. Lin, Y.; Tronche, E.J.; Steenstra, E.S.; van Westrenen, W. Experimental constraints on the solidification of a nominally dry lunar magma ocean. *Earth Planet. Sci. Lett.* **2017**, *471*, 104–116. [[CrossRef](#)]
61. Rapp, J.F.; Draper, D.S. Fractional crystallization of the lunar magma ocean: Updating the dominant paradigm. *Meteorit. Planet. Sci.* **2018**, *53*, 1432–1455. [[CrossRef](#)]
62. Snyder, G.A.; Taylor, L.A.; Neal, C.R. A chemical model for generating the sources of mare basalts: Combined equilibrium and fractional crystallization of the lunar magmasphere. *Geochim. Cosmochim. Acta* **1992**, *56*, 3809–3823. [[CrossRef](#)]
63. Xu, M.; Jing, Z.; Van Orman, J.A.; Yu, T.; Wang, Y. Experimental Evidence Supporting an Overturned Iron-Titanium-Rich Melt Layer in the Deep Lunar Interior. *Geophys. Res. Lett.* **2022**, *49*, e2022GL099066. [[CrossRef](#)]
64. McGovern, P.J.; Litherland, M.M. Loading Stresses and Magma Ascent In and Around Large Lunar Impact Basins: Scenarios for the Emplacement of Mare Basalts. In Proceedings of the 41st Annual Lunar and Planetary Science Conference, The Woodlands, TX, USA, 1–5 March 2010; p. 2724.
65. Solomon, S.C.; Head, J.W. Vertical movement in mare basins: Relation to mare emplacement, basin tectonics, and lunar thermal history. *J. Geophys. Res. Solid Earth* **1979**, *84*, 1667–1682. [[CrossRef](#)]
66. Zhang, N.; Ding, M.; Zhu, M.-H.; Li, H.; Li, H.; Yue, Z. Lunar compositional asymmetry explained by mantle overturn following the South Pole–Aitken impact. *Nat. Geosci.* **2022**, *15*, 37–41. [[CrossRef](#)]

**Disclaimer/Publisher’s Note:** The statements, opinions and data contained in all publications are solely those of the individual author(s) and contributor(s) and not of MDPI and/or the editor(s). MDPI and/or the editor(s) disclaim responsibility for any injury to people or property resulting from any ideas, methods, instructions or products referred to in the content.